*The 2023 World Congress on*
***Advances in Structural Engineering and Mechanics (ASEM23)***
*GECE, Seoul, Korea, August 16-18, 2023*

# Fatigue performance and a unified fatigue crack growth model of ASTM A709 grade 50 steel

*Wen-Cheng Yeh[1)] and Yung-Ming Wang[2)]

[1)] *Department of Civil Engineering, NPUST, Pingtung 912-301, Taiwan*
[2)] *Department of Civil Engineering, NCKU, Tainan 701-01, Taiwan*

[1)] *weyeh@mail.npust.edu.tw*

## ABSTRACT

As A709 steel is widely adopted in bridge engineering, the fatigue behavior will be also an important issue during service life. The fatigue crack behavior of A709 GR50 were investigated in this study. Both the fatigue test and unified fatigue crack growth model will be presented in this paper. First, the fatigue test will be carried out with CT (compact tension) specimens made and different stress ratio will be considered for cyclic loading of fatigue test. The rate of crack growth per cycle versus to stress intensity factor (SIF) range will be plotted from the fatigue test data of CT specimens, where the crack length will be evaluated with compliance method according to the crack opening displacement (COD). Hence, we can obtain the fatigue crack growth rate (FCGR) and the SIF range under different maximum loading and stress ratios.

The FCGR curves with a double-logarithmic scale show that stage II, the dominant stage during the fatigue crack life, exhibits linear and colinear for different stress ratio within the specified maximum loading. Besides, the center points of the stage II move in proportion to the stress ratio. By regression analysis and scaling of the FCGR curves, a unified fatigue crack growth model can be developed with a quintic polynomial to simulate FCGR of A709 GR50 steel under different stress ratio within the same maximum loading. The effectiveness of this study and its performance are also shown through the comparison of relationship between crack length and numbers of cyclic loading predicted by the present unified model with the experiment data.

## 1. INTRODUCTION

[1)] Associate Professor
[2)] Associate Professor

Steel structures are widely used in bridge engineering due to their ease of assembly, precise control, excellent ductility, high toughness capacity, and superior seismic performance in (Tang 2022). A709 GR50 is one of the most commonly used steels in current highway bridge construction in Taiwan. A709 GR50 has a specified yield strength of 345 MPa and is suitable for manufacturing structural components with a thickness of 2-16 millimeters. During the service life, highway bridges are subjected to cyclic dynamic loads caused by vehicular traffic, particularly at stress and geometric discontinuities where stress concentration phenomena occur. This can lead to the formation of cracks and fatigue issues, ultimately resulting in fatigue failure of the steel structure by (Wang 2019). Therefore, studying the fatigue performance of A709 GR50 steel is crucial for fatigue assessment and the safe design of steel structures.

The fatigue crack growth rate (FCGR) has a crucial impact on predicting the fatigue life and designing damage tolerance of materials. In general, for metallic materials with an initial crack, the fatigue life can be divided into three regions of the FCGR curve, namely the threshold region (Region I), stable growth region (Region II), and unstable growth region (Region III). (Hu 2019) have demonstrated that for materials with an initial crack, the fatigue life is primarily governed by Region II, indicating that the total residual fatigue life of the material is almost entirely consumed in this region. Therefore, if the FCGR formula can be established accurately, one can analyze the fatigue life and assess the residual fatigue life of steel structures by integrating the FCGR formulas. This can also conduce engineer to prevent catastrophic accidents caused by fracture failure of steel structures with timely maintenance and replacement.

As we know, the Paris law is primarily used to calculate the FCGR at specific stress ratios and does not consider the effect of the stress ratio.
However, the stress ratio is one of the most important factors affecting the fatigue crack growth behavior of metals materials. Numerous mathematical models, has been proposed to quantify the effect of stress ratio on the FCGR. such as the Walker model (Beden 2009), Forman model (Ribeiro 2021), and Donahue R. J. model (Donahue 1972), The Walker model introduced the parameters related to stress ratio effect into the model to evaluate the influence of stress ratio on the FCGR. Moreover, the Forman model and Donahue R. J model incorporate parameters related to the stress ratio effect, as well as the threshold value $\Delta K_{th}$ and fracture toughness $K_c$. These additional parameters allow for a more comprehensive evaluation of the fatigue crack growth behavior under different stress ratios and provide a better understanding of the crack growth characteristics in various growth stages.

In this paper the fatigue test and unified fatigue crack growth model will be presented. the fatigue test will be carried out with CT (compact tension) specimens made from the A709 GR50 steel and different stress ratio will be considered for cyclic loading of fatigue test. The unified fatigue crack growth model was developed based on the FCGR through fatigue test. The unified fatigue crack growth model of A709 GR50 presented in this study is consistent with the Paris law. Moreover, the unified crack growth model adequately describes the FCGR of A709 GR50 under different stress ratios at the same maximum load. Therefore, this model can not only estimate the FCGR under different stress ratios but also establish a crack growth predictive model to predict crack growth.

## 2. Fatigue test

### *2.1. Material, specimens design and Fatigue experiment program*

The structural steel investigated in this study is A709 GR50, which is widely used for bridges in Taiwan. According to ASTM, A709 GR50 indicates that the steel has a nominal minimum yield strength of 345 MPa and a minimum tensile strength of 450 MPa at room temperature. The fatigue test for the A709 GR50 steel is typically performed according to a standardized test method, ASTM E647 (2015), which specifies the procedures for specimen preparation, loading, and data analysis. In this paper, CT (Compact Tension) specimens made from the A709 GR50 steel were adopted to evaluate the resistance to fatigue crack growth under cyclic loading conditions. The specimens were machined in accordance with ASTM E647 (2015), that is, the CT specimens had to been machined with an electric spark cutting, and the notch direction also was parallel to the rolling direction of steel plate. The geometric details of CT specimens are shown in Fig. 1. The thickness B and width W of all specimens are 5 mm and 50 mm, respectively.

As shown in Fig. 2, the test set-up for FCG were conducted on a Taiwanese brand, Hun-Ta 9707 servo-hydraulic testing machine with a sinusoidal waveform at a frequency of 20 Hz. The FCG test of A709 GR50 steel will be conducted with constant amplitude cyclic loading conditions under different maximum loading, including 30kN, 20 kN, and 24 kN, respectively. In addition, the following stress ratio, 0.1, 0.2, 0.4 and 0.5, will also be considered for the loading conditions. In fatigue testing, the crack growth curve and crack growth rate of CT specimens are primarily determined through the cyclic loading process. The COD of CT specimens corresponding to peaks and troughs during cyclic loading will be measured by cod gauge and logged into a txt file automatically. That is the crack opening displacement (COD) is recorded by crack opening displacement gauge (COD gauge), and then the crack length is calculated by the compliance method. The compliance method involves calculating the crack length based on the recorded COD, taking into account the material properties and specimen geometry. The crack growth length, *a*,and the number of loading cycle *N* curves can be obtained. Also, the SIF amplitude, $\Delta K$, and FCGR can be calculated from (*a*, *N*) data. The Δ*K* can be calculated by the following equations:

$$K_{\mathrm{I}} = \frac{\Delta P}{B\sqrt{W}} f(\alpha) \tag{1}$$

$$f(\alpha) = \frac{(2+\alpha)}{(1-\alpha)^{3/2}} [0.886 + 4.64\alpha - 13.32\alpha^2 + 14.72\alpha^3 - 5.6\alpha^4] \tag{2}$$

where $\Delta P = P_{max}-P_{min}$, $\alpha$ = a/W, a and W represent crack length and CT specimen width, respectively; B is thickness of CT specimen.

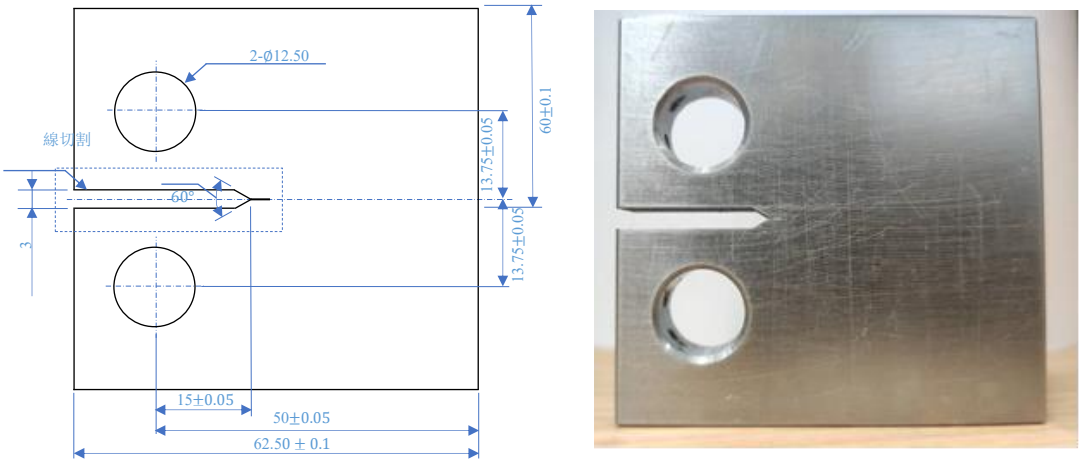


(a) (b)

Fig. 1 Compact tensile specimen (units in mm): (a) detail size of CT specimen; (b) photo of the CT specimen for the fatigue test

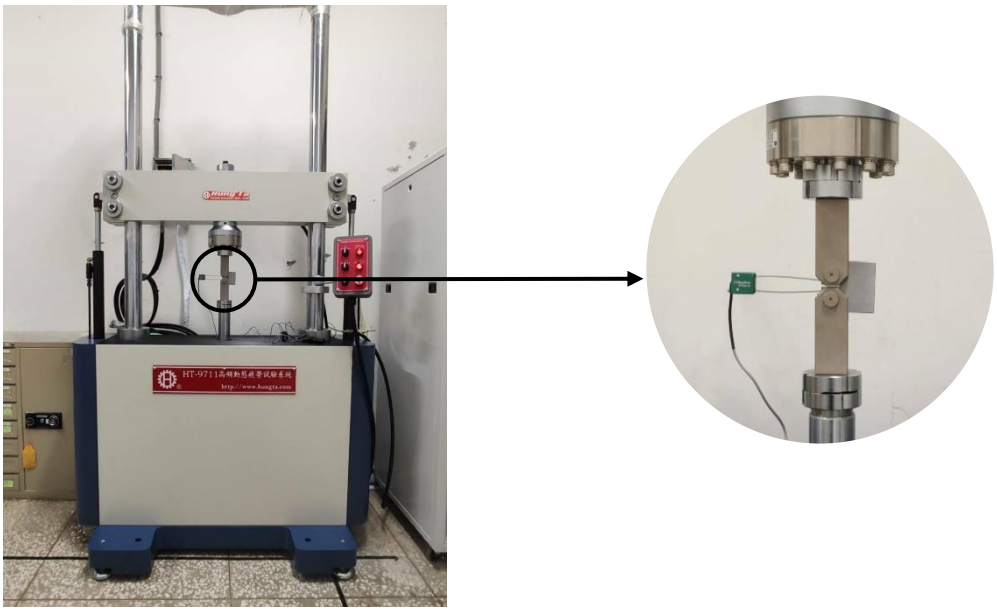

(a) (b)

Fig. 2 Fatigue test diagram: (a) servo-hydraulic testing machine; (b) fatigue crack growth test set-up

*2.2 data capture and smoothing*

As mentioned earlier, fatigue tests involve measuring the COD during each cyclic loading and the crack length is calculated based on it. However, there may be slight variations in the maximum and minimum peaks of each cycle during cyclic loading. It results that the crack length may exhibit oscillations, while the COD is continuously recorded with each loading cycle during fatigue test. Therefore, data capture and smoothing will be an important issue to ensure the COD and crack length can be accurate to calculate the crack growth curve and crack growth rate correctly. Usually, it is common to measure the COD with a certain crack growth increment and then the crack length was calculated on the basis of COD. One percent of crack length is suggested to be crack growth increment by ASTM E647 standard. However, relying solely on a single-point measurement of the COD can be susceptible to errors.

In this study we adopted zero point seven five percent of crack length as crack growth increment. While the crack length obtained through COD and compliance method reaches the specified increment, the crack length will be regard as data sampling point. And a total of 50 points, including 35 points before and 15 points after the reference data point, are taken to proceed numerical smoothing and a cubic polynomial is adopted to fit. That is, the crack length corresponding to these 50 points, obtained by the compliance method based on COD, is approximated with a cubic polynomial regression analysis. The constant term of the resulting polynomial will be taken as the crack length of this sampling point. In this way, the influence of crack growth within a certain number of load cycles before and after the sampling point can be adequately considered. As shown in Fig. 3, the crack length obtained by present method and by compliance method based on continuously COD recording were plotted versus the number of cyclic loading, respectively.

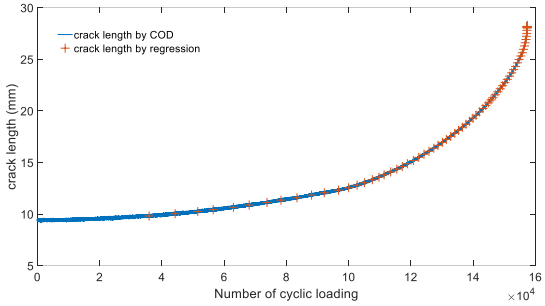


Fig. 3 Crack length versus number of cyclic loading

*2.3 calculation of fatigue crack growth rate (FCGR)*

Based on the specified crack increment and the following previously described method for crack length, the crack growth rate Da/DN can be calculated using the obtained crack length and the corresponding number of load cycles. In this study, the calculation method for Da/DN involves 11 data points for each crack length, which includes 5 data points before and after the target point. These 11 data points, consisting of crack length and corresponding load cycles, are then fitted by a quadratic polynomial. The coefficient of the linear term in the resulting quadratic function is considered as the crack growth rate Da/DN corresponding to the crack length of target point.

Similarly, a quadratic polynomial also adopted to fit SIF amplitude, $\Delta K$ and its corresponding load cycle while calculating the SIF amplitude. The constant term of the quadratic function obtained is considered as $\Delta K$ at that point. This allows us to determine the crack growth rate of each crack length. As shown in Figs. 4-6, the FCG life and FCGR curves of steel A709 GR 50 with different stress ratios under specified maximum loading, including 20 kN, 24 kN and 30 kN were given, respectively.

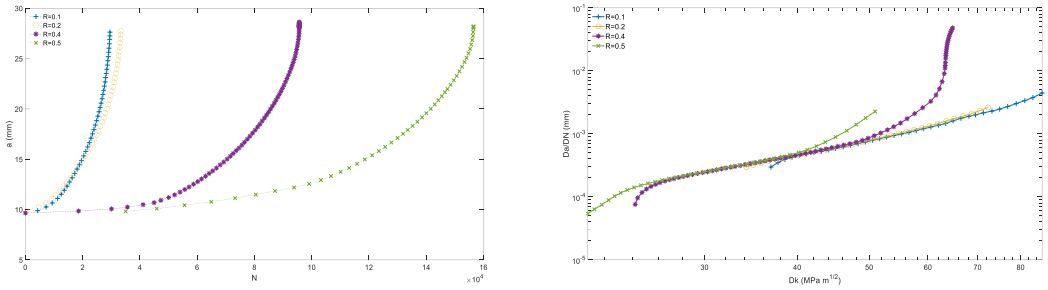


(a) (b)

Fig. 4 FCG life and FCGR curves of steel A709 GR 50 with different stress ratios under maximum loading of 20 kN (a) FCG life curves; (b) FCGR curves.

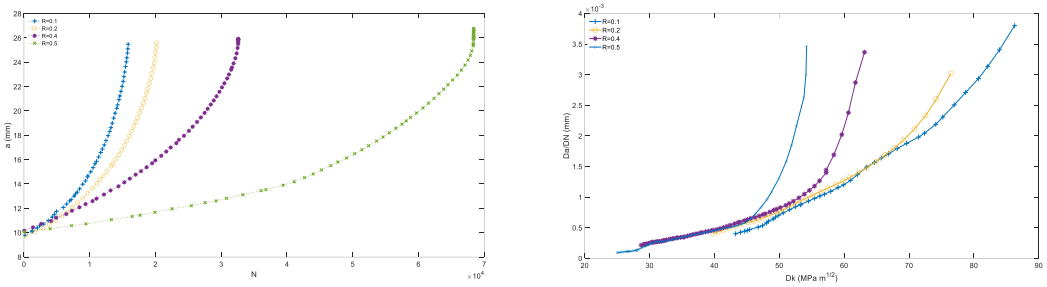


(b) (b)

Fig. 5 FCG life and FCGR curves of steel A709 GR 50 with different stress ratios under maximum loading of 24 kN (a) FCG life curves; (b) FCGR curves.

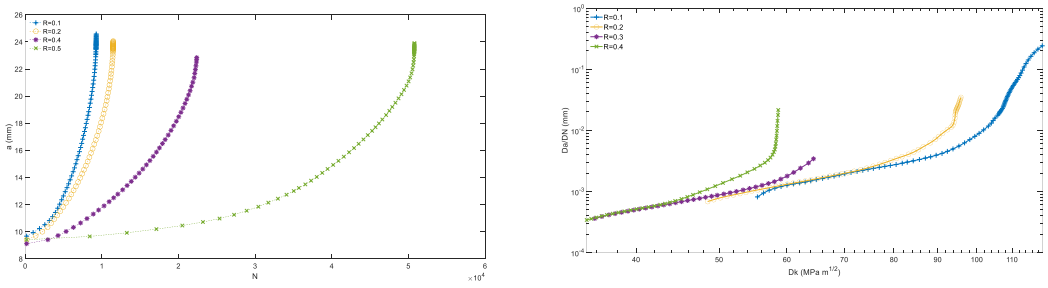


(a) (b)

Fig. 6 FCG life and FCGR curves of steel A709 GR 50 with different stress ratios under maximum loading of 24 kN (a) FCG life curves; (b) FCGR curves.

## 3. unified crack growth model

As shown in Fig. 7 (a), it is found that with different stress ratios under the same maximum loading, the Da/DN-Dk double logarithmic plot exhibits linear in the second segment, and the linear segments of different stress ratio curves are also collinear. This indicates that the second segment of crack growth rate curves of different stress ratios not only has the same slope but also moves on the same line. Therefore, a linear model for the second regions of crack growth rate curves of different stress ratios can be obtained by regression analysis. That is, all crack growth rate curves in the second region of the different stress ratios at the specific maximum loading can be defined with the linear model.

In order to understand the relationship between the linear segment of the crack growth curve and the stress ratio, we can plot the stress ratio versus the corresponding Dk values of the midpoints of the linear segments based on the FCGR curves of different stress ratios. As shown in Fig. 7 (b), it can be observed that the $\Delta K$ of the midpoints of the linear segments in the FCGR curves for different stress ratios decrease proportionally with the stress ratio. Therefore, a linear model can be established through fitting to represent the correlation between $\Delta K$ of the midpoints in the linear segments and the stress ratio. The equation is as shown in Eq. (3). Similarly, we can also determine the relationship between the Da/DN of the midpoints in the linear segments and stress ratio based on the linear model of the Da/DN-Dk second segment. It can be given in Eq. (4)

$$(\Delta K)_R = (\Delta K)_0 + (SdK)(R) \tag{3}$$

$$\left(\frac{da}{dN}\right)_R = \left(\frac{da}{dN}\right)_0 + (Sda)(R) \tag{4}$$

where $(\Delta K)_0$ and $(\Delta K)_R$denote the SIF amplitude at midpoints of the linear segments of the crack growth rate curves with stress ratio 0 and R; $\left(\frac{da}{dN}\right)_0$ and $\left(\frac{da}{dN}\right)_R$ denote the crack growth rate at midpoints of the linear segments on the crack growth rate curves with stress ratio 0 and R; *SdK* is the change rate of the SIF amplitude to stress ratio; *Sda* is the change rate of the crack growth rate to stress ratio.

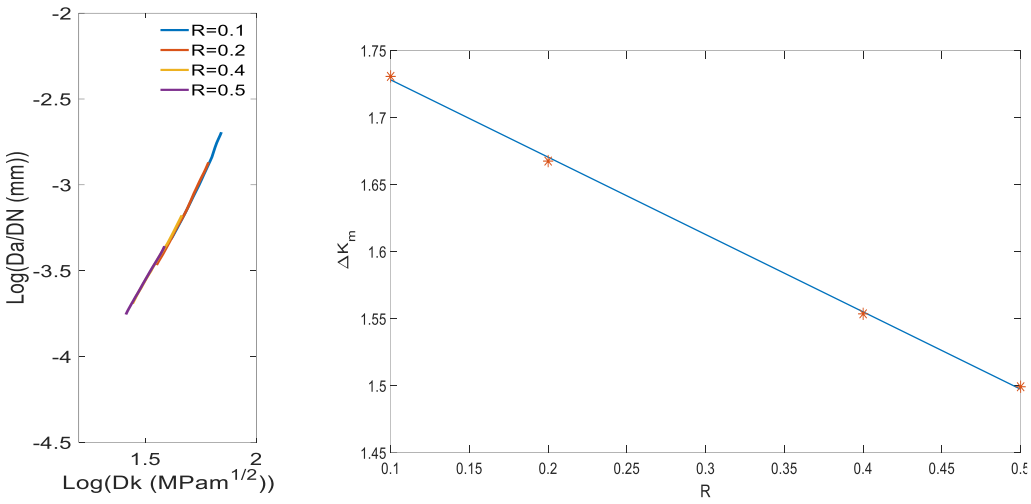


(a) (b)

Fig. 7 Stage II of FCGR curves with different stress ratios under 20 kN: (a) Stage II of FCGR curves; (b) relationship of $\Delta K$ on the midpoints of Stage II versus stress ratio

For convenient comparison, we further shifted all FCGR curves to the position of R=0, based on the previously established linear relationships between Dk and Da/DN of the midpoints in the linear segments with respect to the stress ratio (R). Comparison of the unified curve and FCGR curves with stress ratio R=0 were given in the Fig. 8, it can be seen that the FCGR curves of different stress ratios almost overlap and exhibit consistent trends. Therefore, we can perform regression analysis for all different stress ratio curves to obtain a curve which represent the unified crack growth model under the condition of stress ratio being 0. And in this study a fifth-degree polynomial adopted to fit the shifted curves can give satisfactory results. The equation is given in Eq. (5).

$$\left(\frac{da}{dN}\right)_0 = \sum_{i=0}^{5} C_i \left(\Delta K\right)_0{}^i \tag{5}$$

where $(\Delta K)_0$ and $\left(\frac{da}{dN}\right)_0$ denote the SIF amplitude and crack growth rate at midpoints of the linear segments of the crack growth rate curves with stress ratio 0; $C_i$ is the coefficient of unified curve with stress ratio 0.

Then, the unified crack growth model for different stress ratios under the same maximum loading can be developed through Eq(3), Eq(4)and Eq(5). The comparison of the FCGR curve and unified crack growth model were given in the Fig. 9 (a)-(d). It can be seen that the unified crack growth model is sufficient to adequately describe the FCGR under different stress ratios.

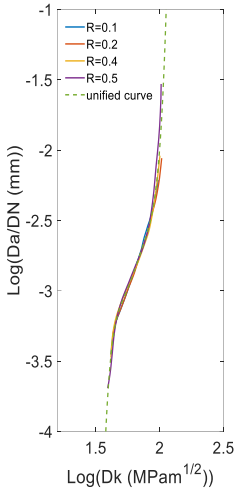


Fig. 8 Comparison of the unified curve and FCGR curves with stress ratio R=0.

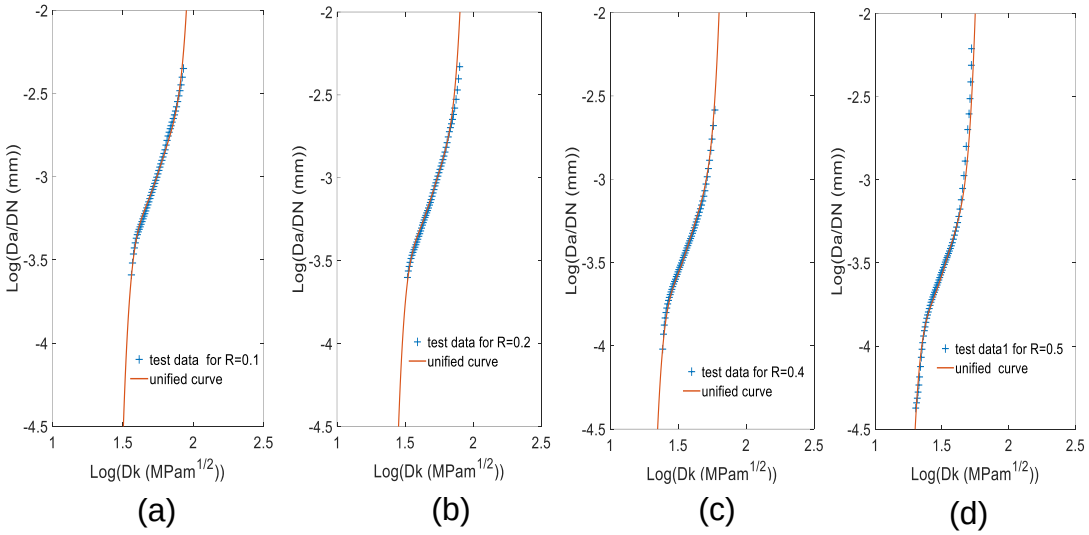


Fig. 9 Comparison of FCGR curves and unified FCGR curves for each stress ratio under 20 kN

## 4. CONCLUSIONS

In this study, the fatigue crack growth test of A709 GR50 steel has been carry out. A data capture and smoothing method, which considers the test data in the vicinity of sampling points and adopt a cubic polynomial to fit, has been developed to determine crack length during cyclic loading. It incorporates the crack growth behavior within a

certain number of load cycles around the sampling point. Then, unified fatigue crack growth model has been developed based on relationship of SIF amplitude and FCGR with different stress ratio, respectively. The effectiveness of this study and its performance are shown through comparisons of the unified crack growth model and the test data with different stress ratios under the specified maximum loading. The present unified crack growth model is capable to describe cyclic loading conditions of different stress ratios under the same maximum loading. However, the unified crack growth model for both different stress ratio and maximum loading can be proceed based on the present study.

## REFERENCES

Tang, Y., Zhu, M., Chen, Z., Wu, C., Chen, B., Li, C., Li, L. (2022), "Seismic performance evaluation of recycled aggregate concrete-filled steel tubular columns with field strain detected via a novel mark-free vision method," Structures, **37**, 426–441.

Wang, B., Nagy, W., Backer, H.D., Chen, A. (2019), "Fatigue process of rib-deck welded joints of orthotropic steel decks," *Theor. Appl. Fract. Mech*., **101**, 113–126.

Hu, X., Zhu, L., Jiang, R., Song, Y., Qu, S. (2019), "Small fatigue crack growth behavior of titanium alloy TC4 at different stress ratios," *Fatigue Fract. Eng. Mater. Struct.*, **42**, 339–351,.

Beden, S.M., Abdullah, S., Ariffin, A.K. (2009), "Review of fatigue crack propagation models for metallic components, *Eur. J. Scientific. Res.,* **28,** 364–397.

Ribeiro, V., Correia, J., Lesiuk, G., Gonçalves, A., Jesus, A.D., Berto, F. (2021), "Application and discussion of various crack closure models to predict fatigue crack growth in 6061–T651 aluminium alloy," *Int. J. Fatigue*, **153**, 106472.

Donahue, R.J., Clark, H.M., Atanmo, P., Kumble, R., McEvily, A.J. (1972), "Crack opening displacement and the rate of fatigue crack growth," *Int. J. Fract. Mech.*, **8** (2), 209–219.

ASTM E647 (2015) Standard Test Method for Measurement of Fatigue Crack Growth Rates.

Hu, X. F., Yao, W.A. (2013) "A new enriched finite element for fatigue crack growth," *Int. J. Fatigue*, **48,** 247-256.